SCRIPTA MEDICA (BRNO) – 79(5–6): 249–260, *December 2006*

COMPUTER SUPPORT FOR EARLY GLAUCOMA DIAGNOSIS BASED ON THE FUSED RETINAL IMAGES

KOLÁŘ R., JAN J., KUBEČKA L.

Department of Biomedical Engineering, Brno University of Technology, Brno

Received after revision November 2006

A b s t r a c t

The autofluorescence of the retinal tissue has a potential to be utilized as a feature for the early glaucoma diagnosis (*3*). In this paper, a new method for detection and segmentation of the zones with a higher level of autofluorescence around the optical disc in autofluorescent images is proposed. Areas of these small isles and their distances from the optical disc (OD) can be used as diagnostic parameters. The border of the OD is determined with the help of auxiliary infrared images, because of higher contrast between OD and surrounding tissue. Consequently, the multimodal registration method of both images to be fused must be applied, relying on our previous results (*14*). The region growing method with manually determined seed points is used for segmentation. We show that the semi-automatic segmentation approach offers a reasonable estimate in comparison with manually segmented regions. The estimate is well defined thus removing the undesirable inter-expert variance.

K e y w o r d s

Autofluorescence, Glaucoma, Image segmentation, Image Registration

INTRODUCTION

The Heidelberg Retina Angiograph (HRA2 – Heidelberg Retina Angiograph) is a kind of scanning laser ophthalmoscope used for angiographic examination of human retina. There are several modes of examination, e.g. fluorescein angiography, ICG angiography, infra-red imaging (*1*). Images that we are interested in here are obtained in autofluorescent (AF) and infrared (IR) mode.

In AF mode, the retina is illuminated by a narrow blue light laser beam (λ=488 nm) in a raster manner. This beam excites the lipofuscin that consequently emits light with a longer wavelength (around 500 nm) (*2*). The emission intensity depends on the amount of lipofuscin accumulation in retinal pigment epithelium (RPE). There are some studies showing the correlation between the lipofuscin accumulations around the optic disc (OD) and the stage of optic disc atrophy (*3*). An example of AF image is shown on *Fig.1 a,b*. The higher level of autofluorescence is predominantly observed at the border of atrophic zone alpha. Histological and electron microscopic investigations demonstrate an accumulation of lipofuscin in lysosomes of the retinal pigment epithelium in this region (*4*).

Progression of parapapillary atrophic zone beta (atrophic zone alpha turns into beta) is correlated with progression of the morphologic (*4,7*) and functional (*8,9*) glaucomatous damage. Histopathological studies have also shown that accumulation of lipofuscin in the RPE is an early feature indicating some disorders already at the time when other ophthalmologic changes are absent (*2*). Therefore, the detection of active parapapillary AF regions, especially in case of ocular hypertension (and possibly glaucoma), may offer an important early diagnosis tool (*3*).

It has been shown that certain geometric parameters (distance and area) of these AF regions can assist the glaucoma diagnosis (*3*). Standard HRA software allows quantitative assessment of local autofluorescence, but the image analysis requires manual outlining of interesting structures. Results of this procedure are subjective to a certain degree. Intraobserver variability has been shown relatively low, but interobserver variability is rather wide even if the assessment is performed by experienced ophthalmologists.

In IR mode, HRA device uses infrared laser light with wavelength 820 nm to illuminate the tissue in raster manner. The reflections are acquired and the IR image has the same size and resolution as the AF image. An example of IR image is shown on *Fig. 1 c.*

The aim of the present work is to semi-automatically determine the borders of all the AF zones in the measured scene, described by the fused image data from both modalities. The method is intended to eliminate the inter-operator variability of segmentation while speeding up the procedure substantially. For each AF zone determined this way, the area and distance from the OD border will be calculated.

MATERIALS AND METHODS

As mentioned above, the AF images contain information about the lipofuscin accumulation in retinal tissue. *Fig. 1 a* and *b* show the whole measured image and close surroundings of the OD with manually segmented AF regions by an ophthalmologist.

In fact, the border of the dark area is not the true OD border, which is inside this area but not clearly visible. That is the reason, why the IR image is used, in which the strong graylevel difference between black spot and the gray surrounding clearly represents the OD border in IR images (*Fig.1c*) and can therefore be well used for OD segmentation.

Because the AF and IR images are recorded in time sequence, the patient (or her/his eye) can move, which causes the spatial movement between the images or even a inside gradually scanned image. To be able to fuse the information from both images, a multimodal registration (*14, 15*) must be performed. This is partly simplified by the same image resolution in both modalities (10 μm/pixel and size 512 x 512 pixels, for low resolution mode and 5 μm/pixel, size 1024 x 1024 pixels, for high resolution mode).

Inside the black area in AF images is the zone beta, which doesn't contain any AF zone (*3*). This zone is peripapillary crescent mostly in the temporal region and becomes circular in more advanced stages. Parapapillary atrophic zone beta is attached to the scleral ring of Elschnig, which represents the optic disc border, and to the zone alpha on the periphery. In fundus color photography the zone beta appears as a grey field on whitish background (*Fig.1d*), with good visibility of large choroidal vessels due to atrophy of retinal pigment epithelium, thinning of chorioretinal tissues and rarification of

choroidal vessels (*5*). The circular extension of AF surrounding from the OD is about 0.14 mm, but in cases with advanced glaucomatous damage this distance is on average 0.24 mm and can reach up to 0.5 mm. The typical area of AF regions ranges from 0.05 mm^2 in normals to 0.24 mm^2 in early and 0.46 mm^2 in advanced glaucomas (*3*).

Our experimental database contains 20 AF and IR images that were all preliminarily manually segmented independently by three experienced ophthalmologists.

Method

Detection of the OD in IR image component

The detection of the OD border is important for two reasons. First, the region of interest must be determined based on the border knowledge. Second, the distance of the AF zones from the optical disc border is expected to be an important diagnostic parameter for glaucoma. We suppose that the center of the OD is known (e.g. manually determined). After image smoothing by an averaging filter, the OD border is initially approximated by the circle with the radius *R*, which minimizes the sum *E* of the pixel value along the circle border *P*:

$$E_{\min} = \min_{R} \sum_{(x,y)\in P} I(x,y) \tag{1}$$

where *I(x,y)* are the graylevel values in the IR image. We are looking for such a circle with radius R, along which the sum of the pixel values is minimal. This can be substantiated as follows: If we examine the IR images, we can see that the OD is always darker then its surrounding (*Fig.1 c*) or *Fig. 2 a,c*) as examples). Although the inner region of the OD is always lighter than the region near its border, this is exluded by the below mentioned limits for R. The circle with the minimal E will therefore approximate the OD border. The radius extent to be searched is determined by the minimal and maximal possible OD size; regarding the resolution, we've used the radius range from 20 pixels to 60 pixels (for 512 x 512 images). These values come from the retinal morphology of the OD.

The active contours (*13*) are consequently used for fine adjustment of the OD border. These curves are based on the cubic B-splines, because of its smoothness (continuous first and second derivatives) and local control (*12*). This ensures the needed stiffness and flexibility for the contour. The evolution of this contour must be controlled by certain image property. The gradient magnitude of the smoothed image was used in our case, because of its good effectivness and easy computation (*13*).

Results of this segmentation are shown on *Fig. 2 a* and *c*. Images *on Fig. 2 b* and *d* are the corresponding AR images incorporating contour from IR image after image registration (see next section).

Image registration

The AF and IR images are taken individually in time sequence, during which the patient (or his/her eye) can move. Therefore, the contour coordinates in IR image may be different from the coordinates of the same detail in AF image, because of the shift and possible distortion between these images. Consequently, a spatial transform *T* that maps the contour coordinates $C_{IR}(x,y)$ from the IR image to coordinates of the AF image $C_{AF}(x,y)$ has to be found. This is done by the multimodal image registration method (*14, 15*), adapted to ophthalmologic images. After successful OD border detection in IR image, this contour must be inserted into to corresponding AF image.

The actual procedure of the registration of AF and IR images consists of three basic steps:

Image preprocessing – for both images, AF and IR, smoothing by anisotropic diffusion (*17*) is performed and gradient images are computed.

Optimization strategy – multiscale approach with controlled random search algorithm is used for registration. As an optimization criterion, the normalized cross correlation (*18*) is utilized in spite of the multimodality. This was possible because of the high correlation of the IR and AF gradient images,

particularly on the edges of the vessels. The optimization provides the transform parameters needed in step 3.

Transform of both images into common coordinates – it has turned out that only rigid transform is sufficient – rotation, scaling and translations in x, y directions are considered.

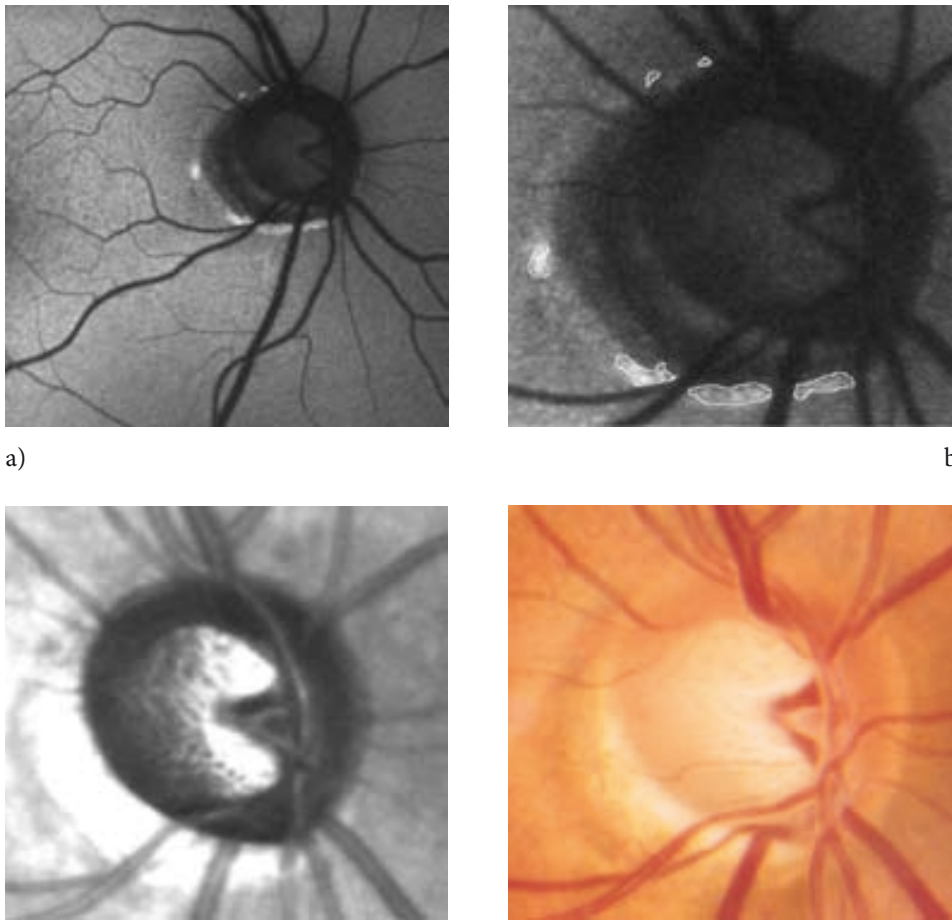

a) b)

c) d)

Fig. 1

The AF image (a) and a detail of the optical disc surroundings (b). The AF zones are visible as bright regions around the black spot. The corresponding IR image (c) and color fundus photography (d)

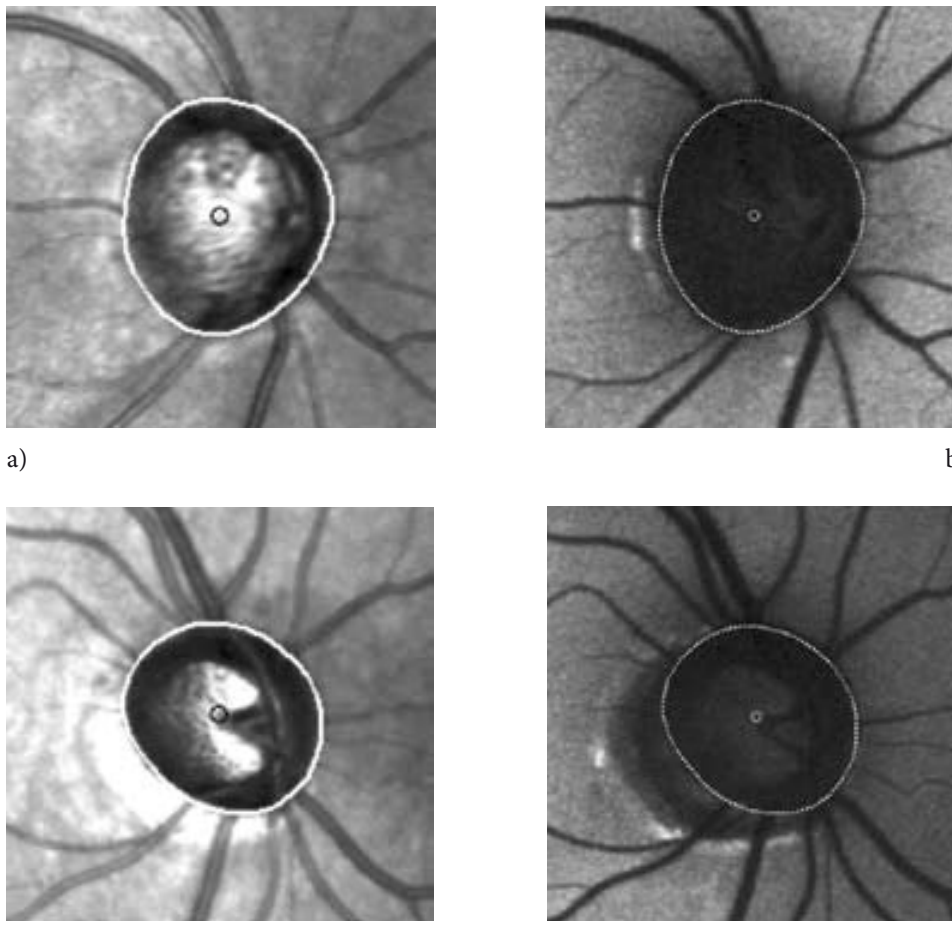

a) b)

c) d)

Fig. 2. a, c
The IR images with detected contour. b,d) Corresponding AF images with incorporated contour.

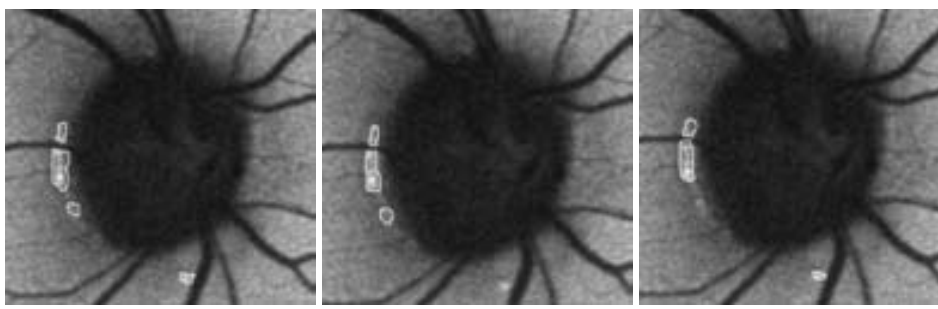

a)

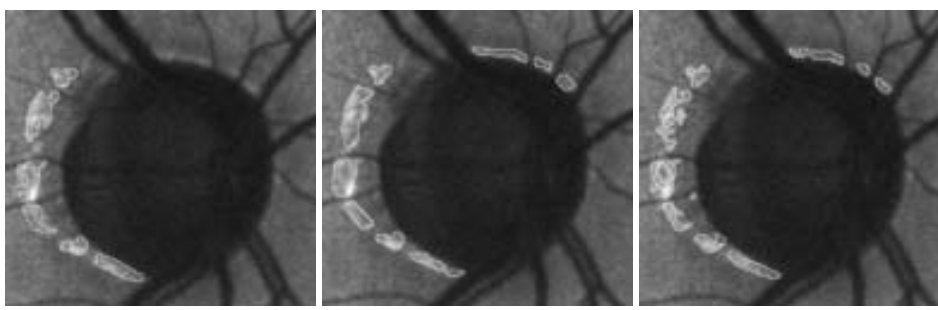

b)

Fig. 3. a

This row presents three images of the same eye segmented by three different physicians. b) Another manually segmented image from our database.

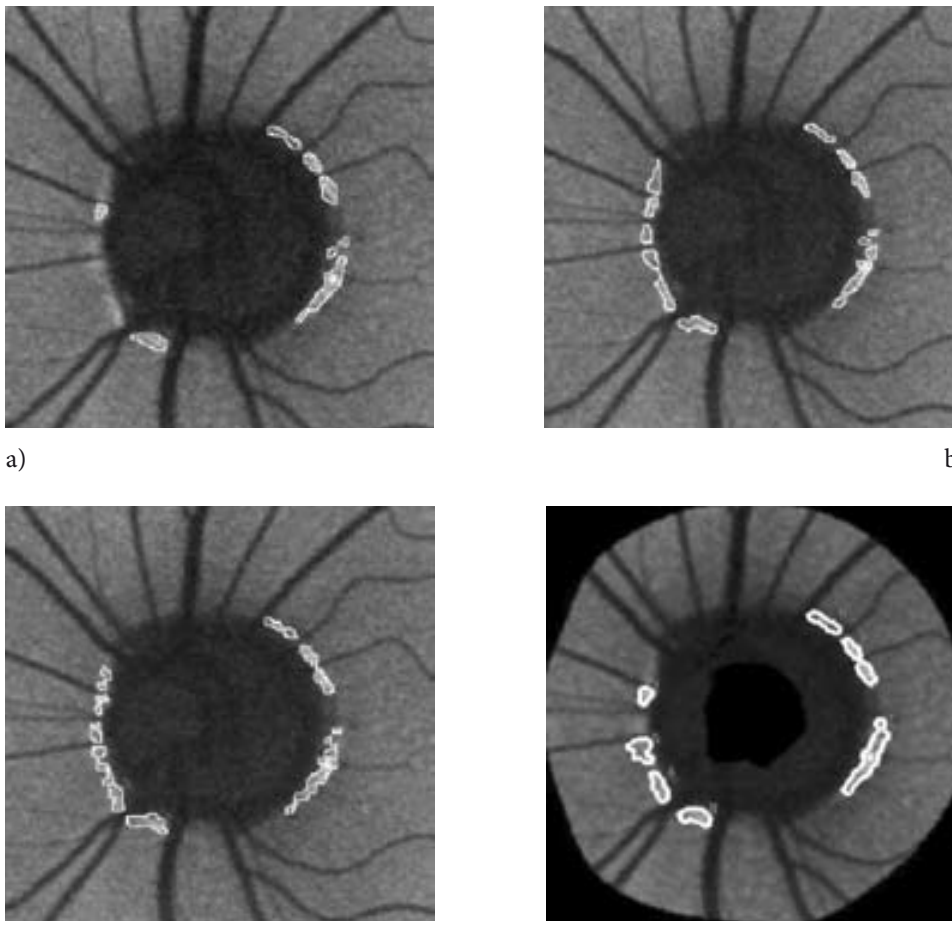

a) b)

c) d)

Fig. 4
Image no. 220. a,b,c) Manually segmented AF regions. d) ROI and segmentation by the proposed method

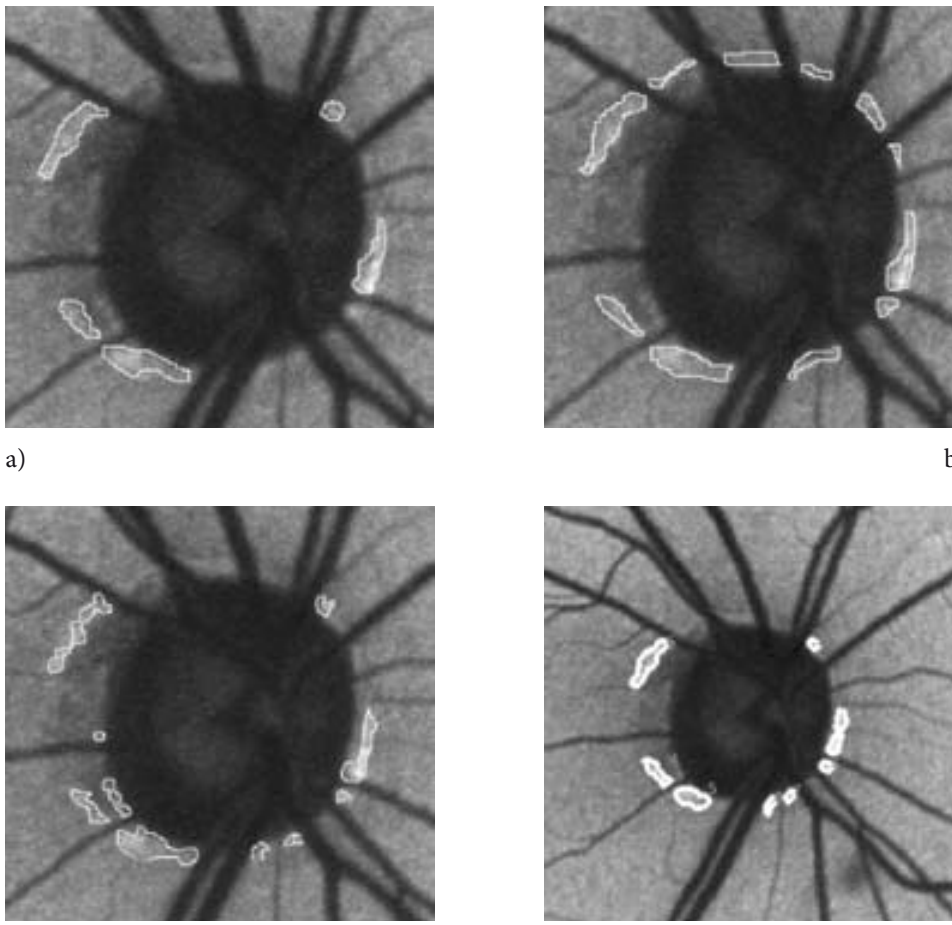

Fig. 5
Image no. 1263. a,b,c) Manually segmented AF regions. d) ROI and segmentation by the proposed method

Semiautomatic segmentation

Fig. 3 shows two AF images with manually segmented AF zones by three different ophthalmologists. A high inter-operator variability can be seen. These examples demonstrate the need for a segmentation method that would eliminate this variability.

Higher accumulation of lipofuscin exhibits itself as small bright isles around the OD and the main feature enabling to recognize them is ther increased brightness in comparison with the background. However, in some cases the contrast is very low. Therefore, our semi-automatic method is based on region growing that compares only the brightness of the region of interest's background (not the whole image) and brightness of currently segmented AF region.

The starting point is manually determined by expert physician. Its position may be slightly autimatcally modified by finding the maximum graylevel value inside a *5* x *5* pixels window around the *user's* seed point to decrease the sensitivity of algorithm to the physician's seed point. During growing, a new candidate point is added to the region when the simple criterion is fulfilled:

$$(RegionMeanValue - CandidatePixelValue) < Threshold. \quad (2)$$

The mean value of the region growing is floating – determined from the so-far accumulated area. The segmentation results depend on the threshold used in region growing method that had to be set experimentally, so that the area border is defined by a relatively high contrast. More details about this approach can be found in (*16*).

RESULTS

It is so far not possible to evaluate the proposed method absolutely, because there is no standard methodology for the AF image segmentation. Therefore, we determined the areas automatically for several AF zones and compared them with the results of expert manual segmentations. *Table 1* shows a simple statistics of the individual areas expressed in pixel count. As can be seen, there are large differences among manually segmented areas. Our method shows a reasonable agreement with the average values of expert segmentation. In case that two or more regions are so close that their border pixels overlap, merging is performed. Several samples of segmentation results are given on *Fig. 4* and *Fig. 5* together with manuall segmentation for comparison.

Table 1
The area of regions (in pixels) for several AF zones in differrent images.

Physician 1	100	346	-	1319	593	121	157	84	96	705
Physician 2	109	469	75	1213	601	63	176	106	126	830
Physician 3	129	371	46	1010	395	36	134	115	110	954
Mean of expert segmentation	**113**	**395**	**61**	**1181**	**530**	**73**	**156**	**102**	**111**	**830**
Our Method	**196**	**442**	**42**	**1208**	**632**	**86**	**125**	**93**	**141**	**776**

DISCUSSION

A new segmentation and analysis methodology of fused AF and IR images leading to support of glaucoma diagnosis has been proposed. It exploits the ophthalmologist's *a priori* knowledge for initialization of the segmentation process. The

advantage of the semiautomatic segmentation over full automatic segmentation is that only valid regions are segmented, based on the expert experience with placing the seed points inside the AF regions, thus preventing the false areas. The method proved to be robust enough with respect to the ophthalmologist's non-exact placement of the seed points. Compared to manual delineation, the computer segmentation I subtatiantly mre time-effective. The obtained values of areas are reasonable approximations of averages manually segmented data. However, more testing in clinical practice will be needed in order to evaluate the diagnostic value and possibility to modify its details.

Acknowledgements

The research was supported in the frame of the DAR – research center no. 1M679855501, sponsored by the Ministry of Education of the Czech Republic and by the Research Programme of Brno University of Technology MSM 0021630513.

The authors would like to thank to Dr. Robert Läemmer and Priv. Doz. Dr. Christian Mardin (Augenklink, Universitätseklinikum Erlangen, Germany) for their valuable comments and for providing the evaluated image data.

Kolář R., Jan J., Kubečka L.

POČÍTAČOVÁ PODPORA PRO VČASNOU DIAGNOSTIKU GLAUKOMU ZALOŽENÁ NA FŮZOVANÝCH OBRAZECH SÍTNICE

Souhrn

Článek se zabývá využitím autofluorescenčních (AF) obrazů sítnice, jako zdroje přídavných informací, pro včasnou diagnostiku glaukomového onemocnění. Je navržen postup pro detekci zón se zvýšenou autofluorescencí v okolí optického disku (OD). Pro každou z těchto oblastí jsou pak určeny dva příznakové parametry – plocha a vzdálenost od hranice OD, které mohou přispět ke stanovení diagnózy. Hranice optického disku je stanovena v infračervených reflexních obrazech sítnice, pořízených laserovým světlem o vlnové délce z oblasti blízké infračervené. Naproti tomu, autofluorescenční oblasti jsou hledány v AF komponentě, vybuzené ultrafialovým laserovým paprskem. Stručně je proto popsán i postup multimodální registrace infračerveného a autofluoescenčního obrazu potřebný pro jejich fůzi. Pro vlastní segmentaci je použita metoda nárustu regionu s manuálním určením startovního bodu. Výhodou poloautomatického přístupu je, že se využívá expertní znalosti oftalmologa pro inicializační umístění startovního bodu a že označení hranice jednotlivých AF oblastí je plně automatické a tudíž časově efektivní. Výsledky jsou porovnány s hodnotami získanými manuální segmentací; je dosaženo rozumného souhlasu parametrů s expertními údaji (s ohledem na jejich rozptyl).

REFERENCES

1. HRA2 information, Internet Site address: http://www.heidelbergengineering.com
2. *Ruckmann A, Fitzke WF, Bird AC.* Distribution of Fundus Autofluorescence with a Scanning Laser Ophthalmoscope. Journal of Ophthalmology. 1995; 79: 407–412.
3. *Viestenz A et al.* In-vivo-Messung der Autofluoreszenz in der parapapillaren Atrophiezone bei Papillen mit und ohne glaukomatose, Optikusatrophie, Klin Monatssbl Augenheilkd. 2003; 220: 545–550.
4. *Kubota T, Schlotzer-Schrehardt UM, Naumann GOH et al.* The ultrastructure of parapapillary chorioretinal atrophy in eyes with secondary angle closure glaucoma, Graefes Arch Clin Exp Ophthalmol. 1996; 234: 351–358.

5. *Jonas JB, Nguyen XN, Gusek GC et al.* Parapapillary chorioretinal atrophy in normal and glaucoma eyes, Invest Ophthalmol Vis Sci. 1989; 30: 908–918.
6. *Kubota T, Jonas JB, Naumann GOH.* Direct clinico-histological correlation of parapapillary chorioretinal atrophy, Br J Ophthalmol. 1993; 77:103–106.
7. *Rockwood EJ, Anderson DR.* Acquired peripapillary changes and progression in glaucoma, Graefes Arch Clin Exp Ophthalmol. 1988; 226:510–515.
8. *Jonas JB, Grundler AE.* Correlation between mean visual field loss and morphometric optic disk variables in the open-angle glaucomas. Am J Ophthalmol. 1997; 124:488–497.
9. *Kono Y, Zangwill L, Sample PA et al.* Relationship between parapapillary atrophy and visual field abnormality in primary open-angle glaucoma. Am J Ophthalmol. 1999; 127: 674–680.
10. *Schweitzer D, Hammer M, Schweitzer F et al.* In vivo measurement of time-resolved autofluorescence at the human fundus. J Biomed Opt. 2004; 9: 1214–1222.
11. *Schweitzer D, Kolb A, Hammer M.* Time-correlated measurement of autofluorescence. A method to detect metabolic changes in the fundus. Ophthalmologe. 2002; 99:774–779.
12. *de Boor C.* A practical guide to Spline. Springer-Verlag, New York, 1978.
13. *Maar D. Hildreth E.* A theory of detection. Proc. Royal Society (London) 1980; B207:187–217.
14. *Kubecka L, Jan J.* Method for Registration of Multimodal Images of Human Retina. Proceedings of 17th Biennial Int. Conf. Biosignal 2004; 255–257.
15. *Kubecka L, Jan J.* Registration of Bimodal Retinal Images – improving modifications. Proc. 26th Internat. Conf. IEEE-EMBS 2004; 1695–1698.
16. *Kolář R, Jan J.* Autofluorescence areas detection in HRA images. IFMBE Proceedings. The 3rd European Medical and Biological Engineering Conference EMBEC 2005, 2384–2388.
17. *Weickert J.* Application of nonlinear diffusion in image processing and computer vision. Acta Math. Univ. Comenianae 2001; 33: 33–50.
18. *Zitova B., Flusser J.* Image Registration Methods: a survey. Image and Vision Computing Elsevier 2003; 21: 977–1000.